Hindawi Publishing Corporation
Journal of Nanomaterials
Volume 2016, Article ID 2710858, 8 pages
http://dx.doi.org/10.1155/2016/2710858

Research Article

Improved Biocompatibility of Novel Biodegradable Scaffold Composed of Poly-L-lactic Acid and Amorphous Calcium Phosphate Nanoparticles in Porcine Coronary Artery

Dongsheng Gu,[1] Gaoke Feng,[2] Guanyang Kang,[3] Xiaoxin Zheng,[2] Yuying Bi,[4,5] Shihang Wang,[4,5] Jingyao Fan,[6] Jinxi Xia,[3] Zhimin Wang,[3] Zhicheng Huo,[3] Qun Wang,[3] Tim Wu,[4,5] Xuejun Jiang,[2] Weiwang Gu,[1] and Jianmin Xiao[3]

[1]*Institute of Comparative Medicine and Animal Center, Southern Medical University, Guangzhou 510282, China*
[2]*Department of Cardiology, Renmin Hospital of Wuhan University, Wuhan 430060, China*
[3]*Department of Cardiology, The Affiliated Dongguan Hospital, Jinan University School of Medicine (The Fifth Renmin Hospital of Dongguan), Dongguan 523000, China*
[4]*VasoTech, Inc., 600 Suffolk Street, Lowell, MA 01854, USA*
[5]*Dongguan TT Medical, Inc., Dongguan 523808, China*
[6]*Emergency & Critical Care Center, Beijing Anzhen Hospital, Capital Medical University, Beijing 100029, China*

Correspondence should be addressed to Weiwang Gu; guww100@163.com and Jianmin Xiao; xiaojianmin0219@163.com

Received 4 December 2015; Accepted 28 February 2016

Academic Editor: Newton M. Barbosa-Neto

Using poly-L-lactic acid for implantable biodegradable scaffold has potential biocompatibility issue due to its acidic degradation byproducts. We have previously reported that the addition of amorphous calcium phosphate improved poly-L-lactic acid coating biocompatibility. In the present study, poly-L-lactic acid and poly-L-lactic acid/amorphous calcium phosphate scaffolds were implanted in pig coronary arteries for 28 days. At the follow-up angiographic evaluation, no case of stent thrombosis was observed, and the arteries that were stented with the copolymer scaffold had significantly less inflammation and nuclear factor-κB expression and a greater degree of reendothelialization. The serum levels of vascular endothelial growth factor and nitric oxide, as well the expression of endothelial nitric oxide synthase and platelet-endothelial cell adhesion molecule-1, were also significantly higher. In conclusion, the addition of amorphous calcium phosphate to biodegradable poly-L-lactic acid scaffold minimizes the inflammatory response, promotes the growth of endothelial cells, and accelerates the reendothelialization of the stented coronary arteries.

1. Introduction

Although metallic drug-eluting stents have dramatically improved the outcome of patients with cardiovascular disease, in-stent restenosis (ISR) and stent thrombosis (ST) remain major challenges [1–4]. Stents are only needed during the vessel healing and reendothelialization periods and, if left in place for a longer period of time, can actually prove harmful by sustaining inflammation, increasing the incidence of ISR and ST, and promoting negative remodeling [5–7]. In this context, stents made of biodegradable polymers such as poly-L-lactic acid (PLLA) appear to be an attractive alternative to durable polymer, as they can be completely replaced by healed tissue and allow positive remodeling [8–13]. However, the poor biocompatibility of PLLA is a major obstacle to its use as a stent component. Indeed, stents made of PLLA have a higher inflammatory potential than metallic stents and are more thrombogenic because of the acidic byproducts released during their degradation. These effects likely promote the development of ISR and the occurrence of ST [12, 14], interfere with the proliferation of endothelial cell, and delay vessel healing [15, 16]. Since the rapid and complete reendothelialization of the stented segment can prevent the occurrence of inflammatory and

thrombotic events, a polymer composite with endothelial cell-positive properties could prove to be of great value for the development of novel stent technologies.

Amorphous calcium phosphate (ACP) is used in the form of coatings, ceramics, and composites in numerous biomaterials and has excellent biocompatibility due to its chemical similarity to human bone tissue [17]. It has been reported that ACP can reduce the inflammatory reaction associated with the hydrolytic degradation of PLLA [9, 10, 18]. When in the human body, ACP releases $P_2O_7^{4-}$ ions into aqueous media, which are hydrolyzed to form hydroxide ions (OH^-). In turn, OH^- then neutralizes the carboxylic acid end group available from the hydrolytic degradation of PLLA. In our previous studies in rats and rabbits, we have reported that the addition of ACP to the PLLA polymer coating significantly improved the biocompatibility of the stent [9, 10]. In this study, we have further investigated the biofunctions of ACP in a biodegradable scaffold consisting of a PLLA/ACP composite when implanted in porcine coronary arteries.

2. Materials and Methods

2.1. Scaffold Preparation. All scaffolds (6 PLLA and 6 PLLA/ACP) were developed and produced by VasoTech, Inc. (Lowell, MA, USA). ACP (size < 150 nm; Ca/P~1 : 1) and paclitaxel were homogeneously mixed with PLLA powder (MW = 250,000 g/mol) with a ratio of PLLA/ACP/PAX at 96/2/2 (w/w/w) using a speed mixer (SpeedMixer™ DAC 600). The mixture was dried at around 60°C overnight prior to extrusion in a single screw extruder (Genca Engineering Inc., Saint Petersburg, FL). For comparison, 2% paclitaxel was also homogeneously mixed with PLLA powder, and the mixture was then extruded under the same condition with PLLA/ACP/PAX extrusion. The extruded tubes have a uniform wall thickness of 150 μm and an outer diameter at 1.8 mm. The extruded tubes were laser-automated according to design specifications (3.0 mm diameter × 13 mm length × 150 μm width). One radiopaque metal marker was incorporated on each end. All scaffolds were crimped on 3.0 mm × 15 mm balloon catheters and sterilized with gamma radiation prior to implantation (Figure 1).

2.2. Animal Preparation and Scaffold Implantation. Twelve Tibetan miniature pigs of either sex and weighing between 20 Kg to 25 Kg were purchased from Pearl River Laboratory (Dongguan, China). The study protocol was approved by the Institutional Animal Care Committee at the Affiliated Hospital of Jinan University, School of Medicine. All procedures involving animals conformed with the "Guide for the Care and Use of Laboratory Animals" published by the US National Institutes of Health (NIH Publication number 85-23, revised 1996).

The implantation procedures were performed as described previously [9]. Briefly, all animals received dual antiplatelet therapy (325 mg aspirin and 75 mg clopidogrel daily) for 3 days prior to the procedure. After a 12-hour fasting period, the animals were anesthetized with 0.3 mg/Kg subcutaneous ketamine and 30–40 mg/Kg intravenous pentobarbital for continuous sedation. A 7F guiding catheter was inserted percutaneously into the coronary artery through the left femoral artery and, after the infusion of 200 μg of nitroglycerin into the coronary artery, quantitative coronary angiography (QCA) was performed from three different views. Tortuous arteries and arteries with diameters <2.5 mm or >3.0 mm were excluded. Each scaffold was implanted randomly in the left anterior descending coronary artery or the right coronary artery (~diameter of 2.8 mm and no obvious tapering, stent to artery ratio 1.1 : 1), slowly expanded to 8 atmosphere (nominal balloon pressure) for 20 seconds before a second QCA was performed. The animals were then given 7,000 U of heparin through the arterial sheath and 200 μg of intracoronary nitroglycerin to prevent vasospasms.

2.3. Follow-Up Quantitative Coronary Angiography and Histopathological Evaluation. At 28 days after implantation, all animals were anesthetized and underwent a follow-up QCA using the same procedures as described above. After the QCA, the animals were euthanized with an anesthetic overdose (4% pentobarbital sodium) and the hearts were harvested, rinsed with 0.9% heparinized saline, and perfusion-fixed with 10% buffered formalin for an hour for histopathological evaluation.

2.4. Quantitative Coronary Angiography Analysis. The QCA analysis was performed offline with a computer-assisted system using an automated edge detection algorithm (MEDIS, Cardiovascular Angiography Analysis System II, Pie Medical Data, Maastricht, NL) by investors blinded to the treatment groups. The segments with the implanted stents were analyzed using two orthogonal views. The proximal luminal diameter (LDp), the distal luminal diameter (LDd), and the middle luminal diameter (LDm) were measured in each stented artery segment. The mean luminal diameter (MLD) was defined as (LDp + LDd + LDm)/3.

2.5. Histology and Immunohistochemistry. All stented arteries were paraffin-embedded and sectioned into 5 μm thick proximal, central, and distal segments. The sections were then stained with hematoxylin-eosin, as described previously [9, 10].

Two stented arteries from two animals were further analyzed with scanning electron microscopy (SEM) to evaluate the degree of reendothelization. For this experiment, the samples were cross-sectioned with a razor blade, and each cross section was sputter-coated with gold-palladium using a desktop gold sputter coater. Photomicrographs were taken using the SEM (VEGA 3, Czech Republic) set at 20 kV.

The inflammation score of each stented segment was graded as described previously: 0, none; 1, scattered inflammatory cells; 2, inflammatory cells encompassing 50% of a strut in at least 25% to 50% of the circumference of the artery; and 3, inflammatory cells surrounding a strut in at least 50% of the circumference of the artery [9, 10]. The endothelialization score was defined as the extent of the circumference of the arterial lumen covered by endothelial

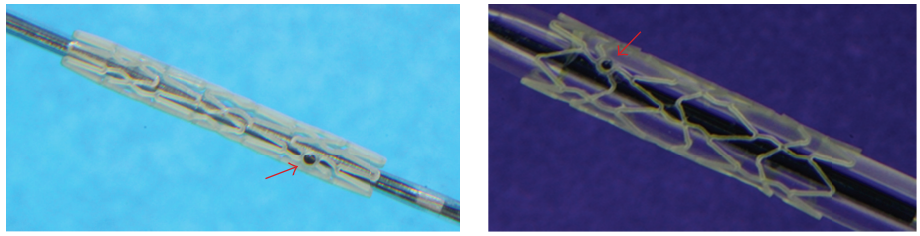

(a) (b)

Figure 1: PowerStent™ Absorb Scaffold. (a) A stent crimped on a balloon catheter. (b) The stent scaffold expanded at 3.0 mm. Red arrows indicate the metal markers at both ends of the scaffold.

cells and graded from 0 to 3 (0 =< 25%; 1 = 25–50%; 2 = 50–75%; and 3 => 75%).

The expression of nuclear factor-κB (NF-κB), platelet-endothelial cell adhesion molecule-1 (PECAM-1), and endothelial nitric oxide synthase (eNOS) was assessed in all stented arteries by immunohistochemistry staining according to the manufacturer instructions (Immunohistochemistry kits, Biosynthesis Biotechnology Co., Beijing, CN). Three individual sections per segment (proximal, central, and distal) were analyzed, and their average was used as a measure of quantification. The percentage of positive cells and the average optical density were analyzed by using Image-Pro Plus 6.0 analysis software (Media Cybernetics, Inc.). The positive expression of the indicator index was defined as the percentage of positive cell × average optical density × 100. The mean value of the proximal, middle, and distal sections was calculated and used as the final measurement for each specimen.

2.6. Blood Sample Assessment. For each animal, 10 mL of coronary arterial blood was withdrawn before the procedure and at 28 days after implantation. The serum concentration of nitric oxide (NO, umol/L) and vascular endothelial growth factor (VEGF, pg/mL) were determined using ELISA kits (Nanjing Jiancheng Biological Engineering Institute, China, and RB Company, USA, resp.) according to manufacturer instructions.

2.7. Statistical Analysis. Statistical analyses were performed with SPSS software version 17.0 (Statistical Product and Service Solutions Ltd.). All data were expressed as mean ± standard deviation (SD), and categorical variables were expressed as counts (%). Independent t-tests were performed to detect between-group differences. All statistical tests were 2-tailed, and a value of $P < 0.05$ was considered statistically significant.

3. Results

3.1. Quantitative Coronary Angiography Analysis. The QCA analysis showed that all 12 scaffolds were successfully deployed at the predetermined diameter, and the stented vessels and the distal branches were open without any sign of peripheral embolization or thrombosis. At 28 days' follow-up, the MLD and percent diameter stenosis were not significantly different between the two groups (Table 1).

Table 1: Coronary angiography measurement at implantation.

Groups	RD (mm)	MLD (mm)	DS (%)
PLLA ($n = 6$)	2.76 ± 0.14	1.94 ± 0.23	29.76 ± 5.46
PLLA/ACP ($n = 6$)	2.78 ± 0.12	2.05 ± 0.20	26.34 ± 5.09
P values	0.84	0.51	0.31

DS: diameter stenosis; MLD: minimal luminal diameter; RD: reference diameter.

3.2. Histology Analysis. At necropsy, gross examination of the hearts showed no coronary abnormalities, epicardial hemorrhage, myocardial infarction, or aneurysms in any of the six PLLA/ACP stented arteries (Figure 2(a)). However, in the PLLA group, one animal had notable tissue inflammation around the stented segment (Figure 2(b)).

Histology evaluation revealed that all scaffolds had neointimal growth present on their surface (Figure 3(a)), and one animal in the PLLA group had notable arterial wall swelling and inflammation (Figure 3(b)). Specifically, SEM showed that the inner layer of the neointima had a rough and textured surface (Figure 4(a)), indicating that the injured intima was not completely healed. In the PLLA/ACP group, the neointima surface was smooth with some endothelial cells immerging (Figure 4(b)), indicating that the reendothelialization process was in progress.

Animals in the PLLA/ACP group had a significantly lower inflammation score (1.20 ± 0.42 versus 1.70 ± 0.48 for PLLA, $P < 0.05$) and higher endothelization score (2.00 ± 0.47 versus 1.40 ± 0.52 for PLLA, $P < 0.05$) (Figure 5(a)).

Immunohistochemistry analysis revealed the positive staining of NF-κB, eNOS, and PECAM-1, among which NF-κB was mainly distributed in the nuclei of the inflammatory cells and eNOS and PECAM-1 were mainly distributed in the nuclei of the endothelial cells (Figure 5(b)). The expression of NF-κB in PLLA/ACP stented arteries was significantly less than that in PLLA stented arteries (22.07 ± 3.18 versus 28.59 ± 3.54, $P = 0.041$) (Figures 6(a) and 6(b)), while the expression of both eNOS (38.53 ± 4.25 versus 27.53 ± 3.55, $P = 0.006$) (Figures 6(c) and 6(f)) and PECAM-1 (29.40±3.84 versus 19.78 ± 3.50, $P = 0.012$) (Figures 6(b) and 6(e)) was

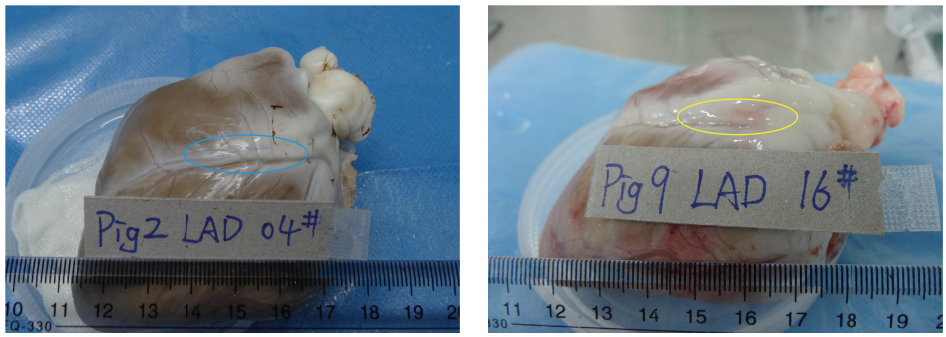

(a) (b)

Figure 2: Gross necropsy examination of the stented hearts. (a) PLLA/ACP scaffold. There are no coronary abnormalities, epicardial hemorrhage, myocardial infarction, and aneurysms (blue circle). (b) PLLA scaffold. Notable tissue inflammation around the stented segment (yellow circle).

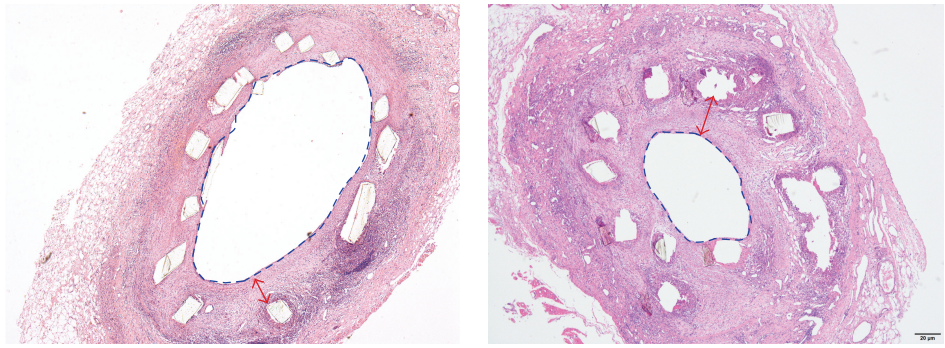

(a) (b)

Figure 3: Histological cross sections of the stented porcine coronary arteries 28 days after implantation (hematoxylin-eosin staining ×4). (a) PLLA/ACP scaffold and (b) PLLA scaffold. Note the remarkable vascular wall swelling, tissue inflammation, and increased neointima thickness (red arrows) and reduced residual area (dashed blue circles) with PLLA scaffold.

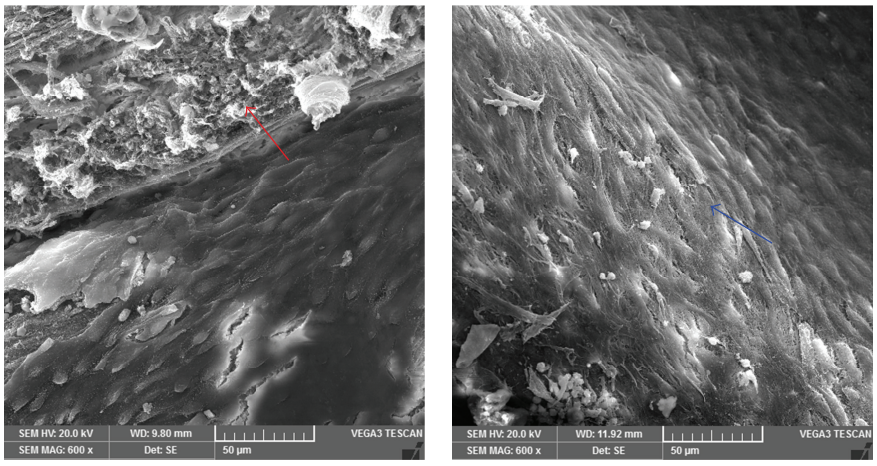

(a) (b)

Figure 4: SEM images of the stented porcine coronary artery vessels 28 days after implantation. (a) PLLA scaffold and (b) PLLA/ACP scaffold. Note the rough, "unhealed" inner vessel wall with PLLA (red arrow) and the smooth, "healed" inner wall with scattered endothelial cell migration with PLLA/ACP scaffold (blue arrow).

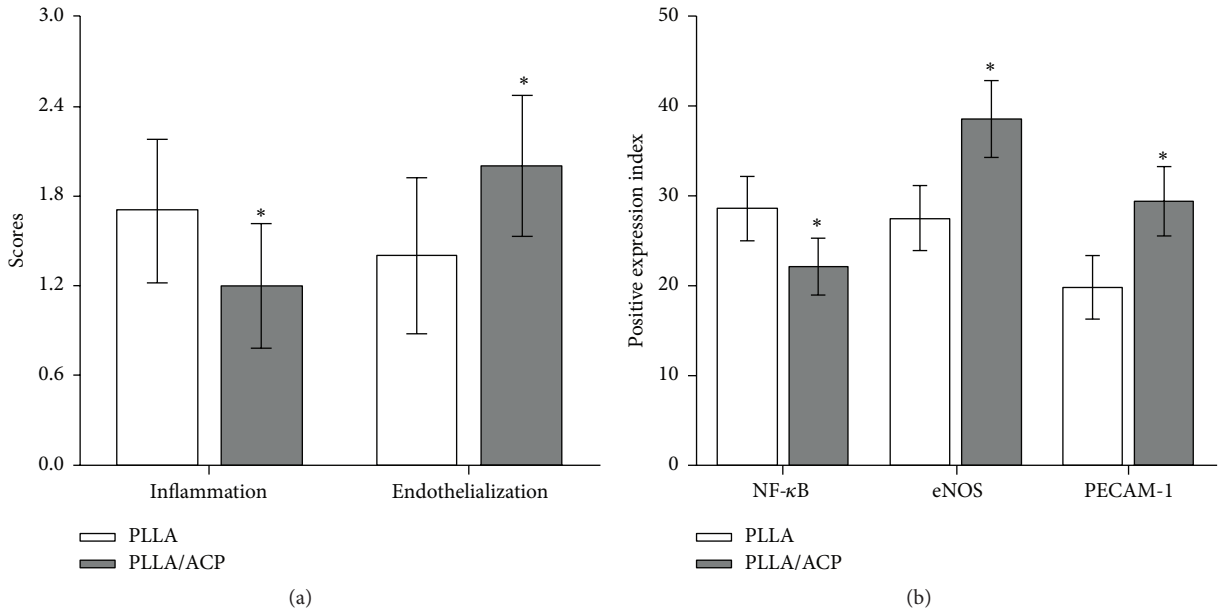

FIGURE 5: (a) The inflammation and endothelial scores 28 days after implantation between the PLLA and PLLA/ACP groups ($^*P < 0.05$). (b) The expressions of NF-κB, eNOS, and PECAM-1 28 days after implantation between the PLLA and PLLA/ACP groups ($^*P < 0.05$).

significantly higher in the PLLA/ACP group than that in the PLLA group.

Compared with the preimplantation values, animals in both the PLLA/ACP and PLLA groups had significantly lower serum concentrations of NO (PLLA/ACP: 176.15 ± 0.63 versus 129.96 ± 9.52, $P < 0.05$; PLLA: 171.85 ± 10.90 versus 79.55 ± 16.5, $P < 0.05$) and higher serum concentrations of VEGF (PLLA/ACP: 205.00 ± 57.88 versus 309.86 ± 49.37, $P < 0.05$; PLLA: 187.81 ± 69.45 versus 222.04 ± 55.16, $P < 0.05$) at 28 days after implantation. In the PLLA/ACP group, both the serum concentrations of NO (129.96 ± 9.52 versus 79.55 ± 16.5, $P < 0.05$) and VEGF (309.86 ± 49.37 versus 222.04 ± 55.16, $P < 0.05$) were significantly higher than that observed in the PLLA group (Table 2).

4. Discussion

The polyester family of polymers, including PLLA, poly-D,L-lactic acid (PDLA), polyglycolic acid (PGA), and poly-lactic-co-glycolic acid (PLGA), have been intensely investigated for biodegradable scaffold platform applications [8, 19–23]. Among these, PLLA was considered a promising candidate with excellent chemical and mechanical properties, but suboptimal biocompatibility has become a major challenge when used as a coating on coronary artery stents [24].

In the present porcine model of coronary artery stenting, both the histopathology and QCA analyses performed at 28 days after implantation showed, with respect to restenosis formation, that the use of a PLLA/ACP composite to generate a fully biodegradable scaffold performed better than when PLLA was used alone. These results are in agreement with our previous studies in rats and rabbits and clearly demonstrate that ACP plays a significant role in improving PLLA biocompatibility and in vivo performance.

4.1. Inhibition of Inflammation. Our histological analyses showed that arteries stented with the PLLA/ACP scaffold had significantly less inflammatory cell infiltration and, consequently, a lower inflammation score. Immunohistochemistry also revealed that the expression of NF-κB was significantly lower in PLLA/ACP stented arteries than in PLLA stented arteries. NF-κB is a protein complex that controls the transcription of DNA and plays a key role in the regulation of cellular responses to stimuli such as inflammation, infection, cancer, and autoimmune diseases [25]. In human atherosclerotic plaques, it has been clearly demonstrated that NF-κB is activated and plays a major role in the upregulation of the proinflammatory and prothrombotic responses within the plaque [26–28]. Our results therefore suggest that ACP can significantly alleviate the tissue inflammatory response caused by the scaffold implantation.

The hydrolytic degradation byproducts of PLLA are lactic acid and its oligomer with –COOH groups at the end, which can induce an inflammatory response. As discussed in our previous reports [9, 10], there are two possible reasons as to the inhibitory potential of ACP on the inflammatory process. First, ACP can produce supersaturated levels of Ca^{2+} and $P_2O_7^{4-}$ ions by releasing ions into the aqueous media. The released $P_2O_7^{4-}$ ions can be further hydrolyzed, generating OH^- ions. When ACP is blended into PLLA and placed in aqueous media, the OH^- ions can neutralize the acidic –COOH groups, thus reducing inflammation. Second, the released Ca^{2+} may also be trapped by –COOH groups to

Table 2: Serum levels of NO and VEGF between the period before operation and 28 days after implantation.

Parameters	PLLA group		PLLA/ACP group		P values
	Before operation	28 days	Before operation	28 days	
NO (μmol/L)	171.85 ± 10.90	79.55 ± 16.55	176.15 ± 20.63	129.96 ± 9.52	0.017
VEGF (pg/mL)	187.81 ± 69.45	222.04 ± 55.16	205.00 ± 57.88	309.86 ± 49.37	0.011

NO: nitric oxide; VEGF: vascular endothelial growth factor.
P values are for comparison between the PLLA group and the PLLA/ACP group at 28 days after implantation.

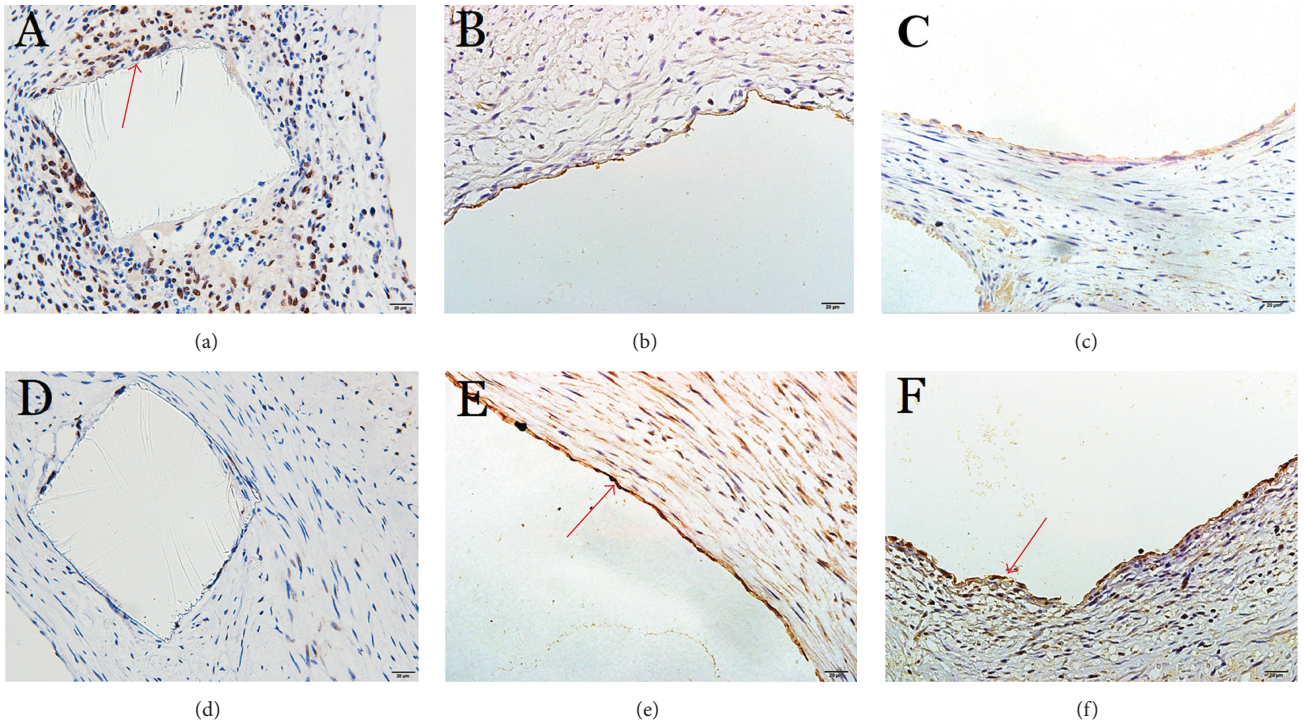

Figure 6: Immunohistochemistry staining of NF-κB (a and d), PECAM-1 (b and e), and eNOS (c and f) positive cells with the PLLA scaffold (a–c) and with the PLLA/ACP scaffold (d–f). The red arrows show positive cells. Note the significantly lower expression of NF-κB in the PLLA/ACP stented artery (d) compared with that of the PLLA stented artery (a) and the significantly higher expression of both eNOS and PECAM-1 in the PLLA/ACP stented artery (e and f) compared to that of the PLLA stented artery (b and c).

form insolubilized salts, providing another possible route to remove the acid.

4.2. Acceleration of Reendothelialization. Studies have demonstrated that delayed arterial healing, characterized by incomplete reendothelialization, is the most powerful histological predictor of ST [5, 29]. Therefore, the presence of a continuous endothelial layer over the stent scaffold will prevent or, at least, diminish the occurrence of thrombotic events. Furthermore, it has been reported that the degree of ISR could be considerably reduced if the endothelium regenerates rapidly and completely after stenting [30].

Platelet-endothelial cell adhesion molecule-1 (PECAM-1) is a structurally important marker for endothelial cells. It mediates cell-cell communication, upregulates the function of integrins, and plays a pivotal role in the transendothelial migration of leukocytes, the regulation of platelet function, the inhibition of apoptosis, and the mediation of signal transduction [31–33]. In the present study, both morphological and morphometric analyses showed that the inner surface of the PLLA/ACP stented arteries had significantly greater endothelial cell coverage than that observed in the PLLA stented arteries. Additionally, our immunohistochemistry analysis revealed that PECAM-1 expression in the PLLA/ACP stented arteries was significantly greater than that of PLLA stented arteries. These results suggest that ACP promotes the growth of vascular endothelial cells and accelerates the reendothelialization process after stent implantation.

Our study also showed that, 28 days after implantation, the expression of eNOS within the vascular wall and the serum concentration of NO were significantly higher in

the PLLA/ACP group than in the PLLA group. Endothelial nitric oxide synthase is mainly distributed in the vascular endothelium and is a key enzyme necessary for the production of NO by endothelial cells [34–36]. Under physiological conditions, eNOS is continuously activated to sustain the constant production of NO by vascular endothelial cells, which is an indicator of endothelial cell integrity. The secreted NO acts as a barrier between endothelial cells and the proinflammatory mediators present in the circulating blood. Because the nanomaterial ACP upregulates the function of eNOS, it may prevent endothelial cell dysfunction following vascular injury as is observed during stenting.

Vascular endothelial growth factor is a highly specific vascular endothelial mitogen, which selectively enhances the mitosis of vascular endothelial cells and degrades the extracellular matrix to allow the migration of endothelial and perithelial cells [37, 38]. By specifically targeting the vascular endothelial cells through the upregulation of A-1 and Bcl-2 expression, it also inhibits endothelial cell apoptosis. At the same time, it upregulates the decay accelerating factor (DAF) to protect endothelial cells from complement-mediated damage and promotes the proliferation of vascular endothelial cells and neovascularization. In the present study, the significantly higher expression of VEGF in the PLLA/ACP group suggests that the addition of ACP to the PLLA scaffold can better facilitate the repair of vascular endothelium.

In addition, because of the addition of nanoscale ACP, the PLLA/ACP scaffolds generate multiple nanopores during the degradation process. This microporous structure provides an excellent surface for cell attachment and possibly a delivery vehicle for cell-based therapies. In this case, blending ACP with PLLA creates nanometer pores that enlarge gradually to a micrometer scale as degradation process could greatly promote the reendothelialization of the injured vessel thereby leading to partial endothelial coverage within 1 month. Therefore, the risk of stent thrombosis is dramatically reduced and, possibly, completely avoided. Compared with the long-term foreign body inflammatory reaction and delayed endothelial repair observed with currently available stents, we believe that the PLLA/ACP scaffold has definitive clinical advantages.

4.3. Limitations and Future Studies. The study was performed in normal porcine coronary arteries, in which the different vascular endothelial repair processes may differ from those observed in atherosclerotic plaques. Also, 28 days of follow-up is short, and because the injured arterial wall is not fully remolded, a study performed using an atherosclerotic model with a longer follow-up period is necessary to fully understand the biological activities of ACP when being part of a PLLA/ACP composite.

5. Conclusion

ACP alleviates the inflammatory response following the implantation of a PLLA scaffold, promotes the growth of endothelial cells, accelerates reendothelialization, and restores endothelial cell structure and function. The addition of ACP to biodegradable scaffolds appears to have a promising future in cardiovascular applications.

Competing Interests

The authors declare that they have no competing interests.

Authors' Contributions

Dongsheng Gu, Gaoke Feng, and Guanyang Kang equally contributed to this work.

Acknowledgments

The study was supported by grants from the Key Program for International S&T Cooperation of China (no. 2011DFA33290 to Weiwang Gu and Tim Wu), the Industrial-Academic Research Collaboration Program of Guangdong, China (no. 2011A091000022 to Weiwang Gu and Tim Wu), the Guangdong Innovative and Entrepreneurial Research Team Program (no. 2014ZT05S008 to Tim Wu and Xuejun Jiang), and the International S&T Cooperation Project of Dongguan, China (no. 2013508150019 to Jianmin Xiao, Tim Wu, Xuejun Jiang, Gaoke Feng, and Guanyang Kang). The authors gratefully acknowledge the help of Chaoshi Qin in analyzing all quantitative coronary angiograms. They thank Weiguo Wan and Lin Xu for the surgical and interventional procedures. Thanks are due to China Scholarship Council.

References

[1] R. Mehran, G. Dangas, A. S. Abizaid et al., "Angiographic patterns of in-stent restenosis: classification and implications for long-term outcome," *Circulation*, vol. 100, no. 18, pp. 1872–1878, 1999.

[2] J. E. Sousa, M. A. Costa, A. Abizaid et al., "Sirolimus-eluting stent for the treatment of in-stent restenosis: a quantitative coronary angiography and three-dimensional intravascular ultrasound study," *Circulation*, vol. 107, no. 1, pp. 24–27, 2003.

[3] M. Joner, A. V. Finn, A. Farb et al., "Pathology of drug-eluting stents in humans: delayed healing and late thrombotic risk," *Journal of the American College of Cardiology*, vol. 48, no. 1, pp. 193–202, 2006.

[4] R. Hoffmann and G. S. Mintz, "Coronary in-stent restenosis—predictors, treatment and prevention," *European Heart Journal*, vol. 21, no. 21, pp. 1739–1749, 2000.

[5] A. V. Finn, G. Nakazawa, M. Joner et al., "Vascular responses to drug eluting stents: importance of delayed healing," *Arterioscle-rosis, Thrombosis, and Vascular Biology*, vol. 27, no. 7, pp. 1500–1510, 2007.

[6] G. Nakazawa, E. Ladich, A. V. Finn, and R. Virmani, "Pathophysiology of vascular healing and stent mediated arterial injury," *EuroIntervention*, vol. 4, supplement C, pp. C7–C10, 2008.

[7] F. Prati, M. Zimarino, E. Stabile et al., "Does optical coherence tomography identify arterial healing after stenting? An in vivo comparison with histology, in a rabbit carotid model," *Heart*, vol. 94, no. 2, pp. 217–221, 2008.

[8] Z. Sun, "Endovascular stents and stent grafts in the treatment of cardiovascular disease," *Journal of Biomedical Nanotechnology*, vol. 10, no. 10, pp. 2424–2463, 2014.

[9] Z. Lan, Y. Lyu, J. Xiao et al., "Novel biodegradable drug-eluting stent composed of poly-L-lactic acid and amorphous calcium phosphate nanoparticles demonstrates improved structural and functional performance for coronary artery disease," *Journal of Biomedical Nanotechnology*, vol. 10, no. 7, pp. 1194–1204, 2014.

[10] X. Zheng, Y. Wang, Z. Lan et al., "Improved biocompatibility of poly(lactic-co-glycolic acid) and poly-L-lactic acid blended with nanoparticulate amorphous calcium phosphate in vascular stent applications," *Journal of Biomedical Nanotechnology*, vol. 10, no. 6, pp. 900–910, 2014.

[11] F. Vogt, A. Stein, G. Rettemeier et al., "Long-term assessment of a novel biodegradable paclitaxel-eluting coronary polylactide stent," *European Heart Journal*, vol. 25, no. 15, pp. 1330–1340, 2004.

[12] W. J. Van der Giessen, A. M. Lincoff, R. S. Schwartz et al., "Marked inflammatory sequelae to implantation of biodegradable and nonbiodegradable polymers in porcine coronary arteries," *Circulation*, vol. 94, no. 7, pp. 1690–1697, 1996.

[13] H. Qiu, X.-Y. Hu, T. Luo et al., "Short-term safety and effects of a novel fully bioabsorable poly-L-lactic acid sirolimus-eluting stents in porcine coronary arteries," *Chinese Medical Journal*, vol. 126, no. 6, pp. 1183–1185, 2013.

[14] A. M. Lincoff, J. G. Furst, S. G. Ellis, R. J. Tuch, and E. J. Topol, "Sustained local delivery of dexamethasone by a novel intravascular eluting stent to prevent restenosis in the porcine coronary injury model," *Journal of the American College of Cardiology*, vol. 29, no. 4, pp. 808–816, 1997.

[15] R. Busch, A. Strohbach, S. Rethfeldt et al., "New stent surface materials: the impact of polymer-dependent interactions of human endothelial cells, smooth muscle cells, and platelets," *Acta Biomaterialia*, vol. 10, no. 2, pp. 688–700, 2014.

[16] N. Kipshidze, G. Dangas, M. Tsapenko et al., "Role of the endothelium in modulating neointimal formation: vasculoprotective approaches to attenuate restenosis after percutaneous coronary interventions," *Journal of the American College of Cardiology*, vol. 44, no. 4, pp. 733–739, 2004.

[17] C. Combes and C. Rey, "Amorphous calcium phosphates: synthesis, properties and uses in biomaterials," *Acta Biomaterialia*, vol. 6, no. 9, pp. 3362–3378, 2010.

[18] D. Skrtic, J. M. Antonucci, and E. D. Eanes, "Improved properties of amorphous calcium phosphate fillers in remineralizing resin composites," *Dental Materials*, vol. 12, no. 5-6, pp. 295–301, 1996.

[19] H. Tamai, K. Igaki, E. Kyo et al., "Initial and 6-month results of biodegradable poly-l-lactic acid coronary stents in humans," *Circulation*, vol. 102, no. 4, pp. 399–404, 2000.

[20] R. Waksman, "Promise and challenges of bioabsorbable stents," *Catheterization and Cardiovascular Interventions*, vol. 70, no. 3, pp. 407–414, 2007.

[21] C. Engineer, J. Parikh, and A. Raval, "Effect of copolymer ratio on hydrolytic degradation of poly(lactide-co-glycolide) from drug eluting coronary stents," *Chemical Engineering Research and Design*, vol. 89, no. 3, pp. 328–334, 2011.

[22] C. Flege, F. Vogt, S. Höges et al., "Development and characterization of a coronary polylactic acid stent prototype generated by selective laser melting," *Journal of Materials Science: Materials in Medicine*, vol. 24, no. 1, pp. 241–255, 2013.

[23] R. Jabara, N. Chronos, O. Hnojewyj, P. Rivelli, and K. Robinson, "Initial assessment of a novel anti-inflammatory bioabsorbable salicylate-based polymer eluting sirolimus for use in fully bioabsorbable coronary stents," *Cardiovascular Revascularization Medicine*, vol. 8, no. 2, pp. 131–132, 2007.

[24] D. F. Williams, "On the mechanisms of biocompatibility," *Biomaterials*, vol. 29, no. 20, pp. 2941–2953, 2008.

[25] T. D. Gilmore, "Introduction to NF-κB: players, pathways, perspectives," *Oncogene*, vol. 25, no. 51, pp. 6680–6684, 2006.

[26] C. Monaco, E. Andreakos, S. Kiriakidis et al., "Canonical pathway of nuclear factor κB activation selectively regulates proinflammatory and prothrombotic responses in human atherosclerosis," *Proceedings of the National Academy of Sciences of the United States of America*, vol. 101, no. 15, pp. 5634–5639, 2004.

[27] J. H. Southerland, G. W. Taylor, K. Moss, J. D. Beck, and S. Offenbacher, "Commonality in chronic inflammatory diseases: periodontitis, diabetes, and coronary artery disease," *Periodontology 2000*, vol. 40, no. 1, pp. 130–143, 2006.

[28] N. S. Rial, K. Choi, T. Nguyen, B. Snyder, and M. J. Slepian, "Nuclear factor kappa B (NF-κB): a novel cause for diabetes, coronary artery disease and cancer initiation and promotion?" *Medical Hypotheses*, vol. 78, no. 1, pp. 29–32, 2012.

[29] A. V. Finn, M. Joner, G. Nakazawa et al., "Pathological correlates of late drug-eluting stent thrombosis: strut coverage as a marker of endothelialization," *Circulation*, vol. 115, no. 18, pp. 2435–2441, 2007.

[30] A. Curcio, D. Torella, and C. Indolfi, "Mechanisms of smooth muscle cell proliferation and endothelial regeneration after vascular injury and stenting: approach to therapy," *Circulation Journal*, vol. 75, no. 6, pp. 1287–1296, 2011.

[31] P. C. Evans, E. R. Taylor, and P. J. Kilshaw, "Signaling through CD31 protects endothelial cells from apoptosis," *Transplantation*, vol. 71, no. 3, pp. 457–460, 2001.

[32] K. Choi, M. Kennedy, A. Kazarov, J. C. Papadimitriou, and G. Keller, "A common precursor for hematopoietic and endothelial cells," *Development*, vol. 125, no. 4, pp. 725–732, 1998.

[33] S. M. Albelda, W. A. Muller, C. A. Buck, and P. J. Newman, "Molecular and cellular properties of PECAM-1 (endoCAM/CD31): a novel vascular cell-cell adhesion molecule," *Journal of Cell Biology*, vol. 114, no. 5, pp. 1059–1068, 1991.

[34] S. Lamas, P. A. Marsden, G. K. Li, P. Tempst, and T. Michel, "Endothelial nitric oxide synthase: molecular cloning and characterization of a distinct constitutive enzyme isoform," *Proceedings of the National Academy of Sciences of the United States of America*, vol. 89, no. 14, pp. 6348–6352, 1992.

[35] Y. Wang and P. A. Marsden, "Nitric oxide synthases: biochemical and molecular regulation," *Current Opinion in Nephrology and Hypertension*, vol. 4, no. 1, pp. 12–22, 1995.

[36] X. F. Figueroa, D. R. González, M. Puebla et al., "Coordinated endothelial nitric oxide synthase activation by translocation and phosphorylation determines flow-induced nitric oxide production in resistance vessels," *Journal of Vascular Research*, vol. 50, no. 6, pp. 498–511, 2013.

[37] N. Ferrara, "Vascular endothelial growth factor," *Arteriosclerosis, Thrombosis, and Vascular Biology*, vol. 29, no. 6, pp. 789–791, 2009.

[38] M. Bry, R. Kivelä, V.-M. Leppänen, and K. Alitalo, "Vascular endothelial growth factor-B in physiology and disease," *Physiological Reviews*, vol. 94, no. 3, pp. 779–794, 2014.